UNIVERSITY OF TWENTE - SCHOOL OF ADVANCED TECHNOLOGY

A Review of Niobium Titanium for Superconducting Purposes

Emma van der Minne, Simo Gabriel
Felix Fritz, Jasper Heijenk, Cham Bustraan

July 5, 2020

REPORT

Abstract

To ensure control over the plasma inside the International Thermonuclear Experimental Reactor superconducting magnets of NbTi are utilized. The goal of this report is to give basic material properties of NbTi and relate them to the fabrication of the material. The information is obtained via a literature search and, when needed, completed with our own insights. First the crystal structure of the material is presented. After that different material properties like mechanical, electrical, magnetic etc. are described and related to the crystal structure. Then the relation between the synthesis and structure of the material is given. And finally there is a comparison with a different promising superconducting material Nb_3Sn.

Contents

1 Introduction

Since the nuclear disaster of Fukushima in 2011, the search for safer and non polluting energy sources just has experienced an even stronger upwind: Looking at Germany, 8 nuclear reactors were shut down immediately after the disaster and by 2022, all of Germany's nuclear reactors will be shut down. Since the government and the nation do not believe in nuclear power in terms of nuclear fission anymore, the focus now lies more on renewable energy, and the switch from nuclear to renewable sources is estimated to cost Germany 1000 Billion Euros[1], where a big part will be spent on research and development. Not only these factors encourage the research on eco friendly projects, but also the growth in the world's population and increase in energy usage per year. That is where nuclear fusion comes into the discussion.

Nuclear fusion describes the principle of fusing two or more light atomic nuclei together, such that they form a new nucleus. During this reaction, a vast amount of energy is released. For nuclear fusion to be a commercially usable energy source, it is required that this released energy is greater than the energy needed to fuse the nuclei.

The reaction takes place in a tokamak, a chamber with magnetic coils, developed in the early 1960's by I. Tamm and A. Sakharov, whose concept was adopted by researchers around the world very quickly.[2] The tokamak acts as a confinement for plasma, which is essentially a gas where a great amount of its molecules are ionized, which makes it possible for the plasma to conduct electric charges. Using these electric charges the plasma can be heated up to around 150 million degrees celsius in the ITER in France, currently the world's largest nuclear fusion project.[4] This is necessary to provide a suitable environment for the fusion reaction to take place. Since no solid material can withstand such high temperatures, the magnetic fields of the coils mentioned earlier are used to control and confine the plasma.

A magnetic field of 11.8 Tesla is needed in ITER for this, made possible by superconducting magnets, which are built from either niobium-titanium or niobium-tin wires. When cooled down to 4 kelvin, NbTi becomes superconducting and can then provide strong magnetic fields. These superconducting magnets are used for the reason that the only energy input has to be the cooling of them to those extremely low temperatures, there is no electrical resistance involved while the current flows through the windings.[6] But of course, there are more superconducting materials than just NbTi, actually almost all metals become superconducting at low temperatures.

The problem with most of them is that a great current or a small magnetic field destruct the superconducting properties, which were already discovered in 1911 by Heike Kamerlingh Onnes in Groningen, Netherlands.[5] A material was needed which can keep up with these challenges, and researchers at Bell Laboratories in the U.S. eventually discovered that Nb_3Sn could sustain high electric super-current densities while having no resistance in great magnetic fields up to 8.8 Tesla. Also around that time, T.G. Berlincourt and R.R.Hake were also interested in superconductors for super-magnetic applications and their work pointed out that while Nb_3Sn fulfills most requirements, it is too brittle and hard to fabricate.

However, after experimenting with different materials, Berlincourt and Hake demonstrated at the 1962 American Physical Society meeting in Washington that niobium-titanium is capable of generating magnetic fields with a strength up to 10 Tesla. This led to NbTi being seen as the workhorse of the superconducting materials.[6]

In this report the focus lies on this specific material; its structure, mechanical, electrical, mag-

netic and optical properties. Furthermore techniques for synthesis are investigated, examined, and their interdepencies made clear.

2 Crystal Structure

Niobium Titanium exists in a body-centered-cubic crystal structure [7]. Because the radii of Nb^{4+} and Ti^{4+} are almost the same, it is expected that this crystal looks like *Fig.* 2.1. This BCC crystal will have a dimension of 0.302 nm when calculated with the ion radius of both Nb^{4+} and Ti^{4+} which are given at 0.069 nm and 0.068 nm respectively. A scientific obtained value is given by 0.329 nm when $Ti_{34}Nb_{66}$ is measured using X-ray.[7] However in NbTi alloys used as superconductor there is also a need for an α-Ti phase, this titanium phase is desired for flux pinning and high critical density, both these properties are explained in more detail below. In high Ti composition of NbTi alloys α-Ti will be distributed over the grain boundaries as well as throughout the grain interiors of the material. This will result in a significant hardening of NbTi.[8] This α-Ti is organized in a hexagonal close-packed crystal structure as also shown in *Fig.* 2.1.[9] An example of a finished NbTi structure where α-Ti is distributed throughout the grains is given in *Fig.* 2.2.[8]

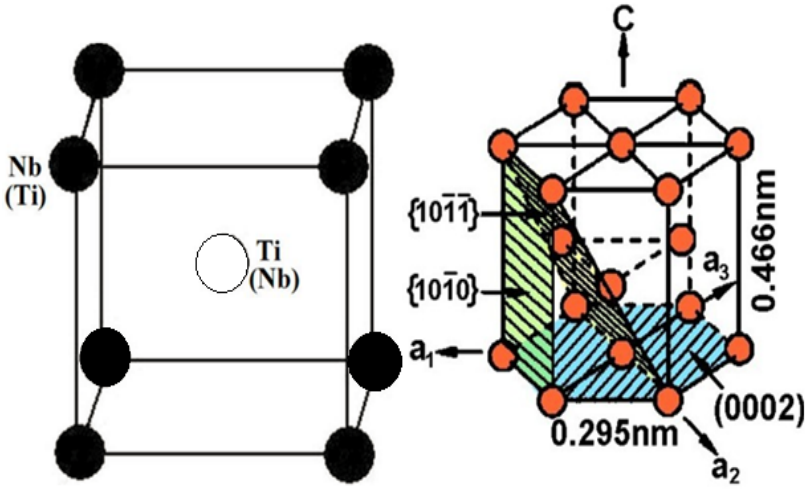

Figure 2.1: Structure of BBC $Nb_{34}Ti_{66}$ (left) and α-phase structure of Titanium (right).

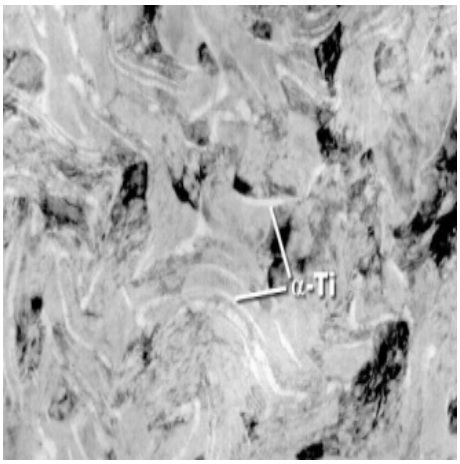

Figure 2.2: Transmission electron microscope image of high critical current density NbTi micro-structure with folded sheets of α-Ti precipitate.

Inside the crystal-structure interactions between the Nb^{4+} and Ti^{4+} ions exist. To get a better idea about how these ions interact we can calculate the energy between the ions. Before one can consider a lattice of ions, first a look at a single pair of oppositely charged ions separated by a distance r should be made.
For the electrostatic attractive energy E:

$$E = -\frac{|Z_m||Z_x|e^2}{4\epsilon_0 \pi r} \tag{2.1}$$

where Z_m and Z_x are the charges on the cation and anion, respectively. The fact that the right term is negative means that as r becomes smaller the energy becomes increasingly more negative. Next to the attractive energy we have the repulsive energy. Because the electronic configuration of Nb and Ti elements are:

- Nb: $1s^2 2s^2 2p^6 3s^2 3p^6 3d^{10} 4s^2 4p^6 4d^4 5s$
- Ti: $1s^2 2s^2 2p^6 3s^2 3p^6 3d^2 4s^2$

For the charged ions with an shortage of 4 electrons we get te electronic configuration of (assuming the 5s configuration has a significant smaller energy level than the 4d level)

- Nb^{4+}: $1s^2 2s^2 2p^6 3s^2 3p^6 3d^{10} 4s^2 4p^6 5s$
- Ti^{4+}: $1s^2 2s^2 2p^6 3s^2 3p^6$

We can assume that the outer orbitals filled with electrons of both ions overlap because we are dealing with high orbital numbers. As a result strong repulsive forces arise because some electrons must jump into a higher energy state in accordance with the exclusion principle. The repulsion energy rises rapidly with decreasing distance between the ions. The repulsive energy can be given by the equation:

$$E = \frac{B}{r^n} \tag{2.2}$$

where B is a constant, and n is known as the Born exponent. This exponent can be found from compressibility data because the resistance of the ions is directly linked to a decrease in r. Larger ions have higher electron densities and hence values of n. The total energy of the ion pair is given by summing the above equation.

$$E = -\frac{|Z_m||Z_x|e^2}{4\epsilon_0 \pi r} + \frac{B}{r^n} \tag{2.3}$$

However in a crystal lattice, all of the ions interact instead of only with their nearest neighbors. The interaction between ions with opposite charge is attractive and is repulsive between ions of like charge. The summation of all these interactions is known as the Madelung constant, A. For the energy in a lattice we now find:

$$E = -A\frac{|Z_m||Z_x|e^2}{4\epsilon_0\pi r_0} \tag{2.4}$$

We can define The Madelung constant as the ratio of the Coulomb energy of an ion pair in a crystal to the Coulomb energy of an isolated ion pair at the same separation. So A is given by:

$$A = \sum -\frac{Z_i Z_j}{|Z_1||Z_2|r_{ij}} \tag{2.5}$$

In three dimensions, the series presents greater difficulty than the linear example. Let us consider the interactions between the central cation and all of the other ions in the cell. Due to electron neutrality requirements in the unit cell, ions located on the cube faces count *1/2*, those on the cell edges count *1/4*, and the corner ions count *1/8*. If we add this factor into the calculation of A we can get to a final answer using *Fig.* 2.3 we get:

$$A = \frac{-(\frac{8}{8})(\frac{16}{16})}{(2\sqrt{3})} - \frac{(\frac{6}{6})(\frac{16}{16})}{(1)} = -1.28 \tag{2.6}$$

This is possible because we only deal with positive ions so all the ions are of the same sign.

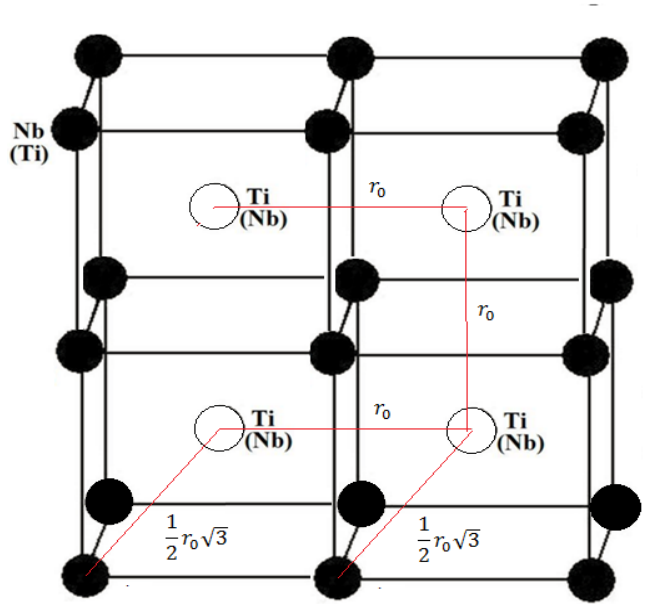

Figure 2.3: NbTi with Ion Distances.

Now with the knowledge of the Madelung constant, the total energy for one mole of the crystal lattice can be written containing an Avogadro number N_a of ion pairs.

$$E = -AN_a\frac{|Z_m||Z_x|e^2}{(4\epsilon_0\pi r_0)}(1-\frac{1}{n}) \tag{2.7}$$

A and r_0 can be derived from the given crystal structure. So with the crystal structure the total energy for one mole of the crystal lattice can be written.

3 MECHANICAL PROPERTIES

In this section of the paper the mechanical properties of NbTi will be discussed. This will include the investigation into the stress-strain behavior of NbTi fibers at room temperature, 77 K, and 4.2 K which yields some unexpected results. Additionally this section will explore the effect of strain rate and cold treatment on the mechanical properties of NbTi.

The amount of stress that a fiber of superconducting NbTi can handle while retaining functionality is of course of major importance as the CICCs in a superconducting magnet used in a design such as ITER are subjected to significant stresses due to the large magnetic fields that the alloy finds itself in. As one might expect the maximum stress that can be applied to a fiber without breaking is dependent on temperature. Usually the lower the temperature of a material the more brittle it is and therefore the less it will stretch before breaking. Contrary to this statement, NbTi strands designed for superconducting purposes do the exact opposite; the lower the temperature it is brought to the larger its maximum strain will be.[10] From *Fig.* 3.1 it can be seen that reducing the strands temperature to 4.2 K more than doubles the maximum stress a strand with a diameter of 18.3 μm can endure as compared to the maximum stress of a strand at 293 K (from about 1.1% to 2.6%).

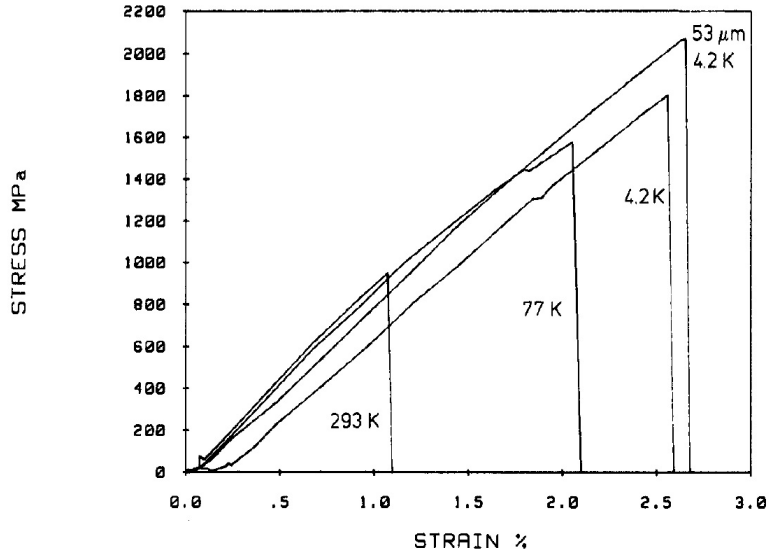

Figure 3.1: Stress-strain graph of 18.3μm diameter strand at 298, 77, and 4.2K[10]

Naturally it is of interest why this highly unusual mechanical-temperature behavior occurs. A fracture stress and fracture strain difference of this magnitude would suggest a different method of fracture for strands at lower temperature. To better understand what is happening SEM photographs of the fractures of the aforementioned 18.3 μm strands at 298 K and 4.2 K are shown in *Fig.* 3.2 and 3.3 respectively. The behavior of the 298 K strand fracture is described as thinning to a flattened cross-section with subsequent partial slant rupture character.[10]

This behavior can be compared with the standard cup-and-cone fracture method.[10] In the cup-and-cone method a small void is formed in the center of strand due to the strain applied to it this void then causes a crack to propagate either upwards or downwards on both sides of the void. The result is that on one side of the fracture is a more concave shape and on the other more convex shape, called the cup and cone respectively. *Fig.* 3.2 has a similar shape as compared to a standard cup with the main difference being the strand has lost its circular shape but

one can still clearly see the cavity that has been left in the center of the strand and the almost parabolic method in which it tapers to the end of the strand.

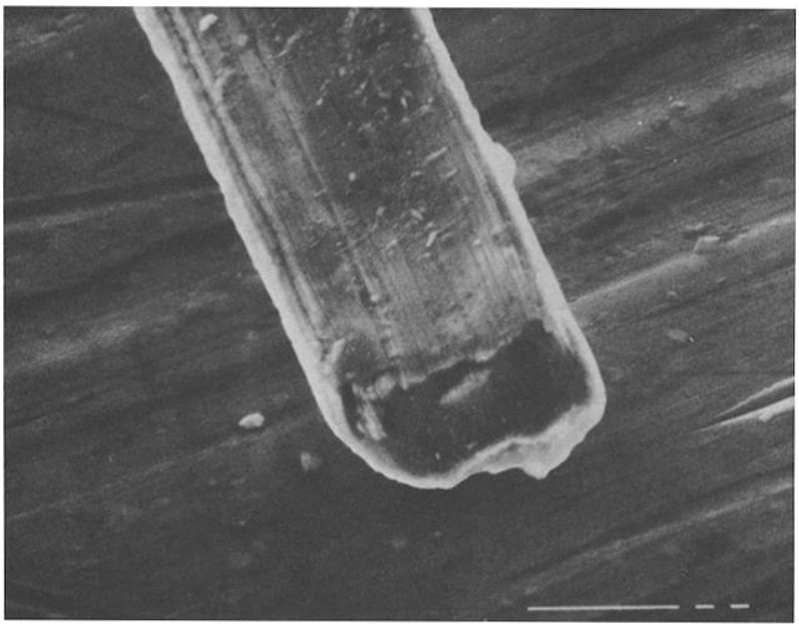

Figure 3.2: SEM photograph of 289K strand fracture [10]

In *Fig.* 3.3 we notice that at lower temperatures the shape of the fracture is different in a number of ways. First of all we notice that on the surface of the fracture there are very many elliptical dimples present on one half of the fracture interface. The second significant difference is that the tapering the NbTi to a point has no longer occurred all around the edges but exists exclusively at the same half of the interface as where the shallow elliptical dimples exist. This definitely does indicate that the fracture method is quite different at very low temperatures. According to the study by Wright, Wiederick, and Hutchison, the elliptical dimple pattern suggests a material of low fracture toughness with impurity sites probably nucleating the shear.[10] They go on to suggest that another reason for the increased fracture strain at low temperatures is due to a discontinuous slip or twinning which extends through the entire strand.

It is conjectured by the writers of this paper based on the above information that as stress is applied to the strand micro-slipping occurs causing only a few crystal layers to be shifted with impurities halting the process for the other layers. As voids begin to occur in the strand the propagation of cracks is halted once again due to the presence of impurities in the alloy. This is why in *Fig.* 3.3 many elliptical dimples can be seen, as many voids had formed before the alloy finally fractured.

Figure 3.3: SEM photograph of 4.2K strand fracture[10]

A superconducting wire however is not just a single strand but rather a bundle of many fibers cladded and encased in copper. Hence, one must also investigate the load-strain of a bundle of NbTi strands as well the effect that the copper cladding has. In *Fig.* 3.4 we see 3 load-strain curves. Curve a shows the response of a bundle of 180 NbTi strands (or in other words the wire without the copper), curve b is the response of the complete superconducting wire, and curve c is the load-strain response of a copper wire with a similar cross section as the superconducting wire. From curve a we see that the bundle of 180 strands does not begin to break until a load of about 55 N is reached, this translates to 0.3 N per strand which corresponds quite nicely with the maximum stress one strand could take before fracture as can be calculated from *Fig.* 3.1. Additionally the first strands fracture at the same strain as found for a single strand. As the bundle of pulled apart further, more and more strands break, as seen by the serrations in the curve, until when it is completely split in two the bundle had elongated a total of roughly 4.5%.

Curve b is the complete superconductor composite response and we can see that the serrating behavior of the bare bundle has disappeared completely due to the copper encasing. The only possible reasons for this can be that surface irregularities (both natural and brought about by the chemical removal of copper to yield the aforementioned strand bundle) of the individual strands have a lesser impact and that the stress is more spread out due to the wire being a more cohesive unit rather than 180 individual fibers. The final strain, however, remains the same at 4.5%. The copper cladding must also serve to raise the load at a fracture by 10 N to 65 N. As a result the copper cladding serves, mechanically speaking, solely as a stabilizer as it were; not actually improving the maximum strain but rather preventing individual NbTi strands from fracturing prematurely.

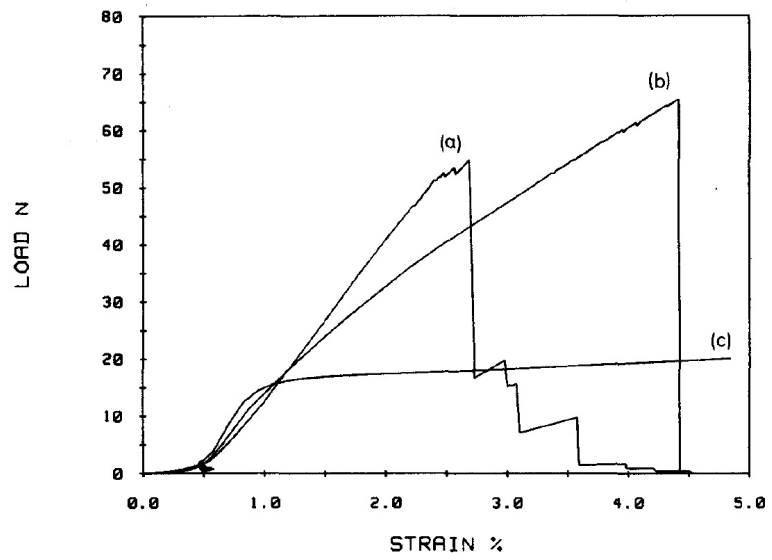

Figure 3.4: Load-strain graph at 4.2K of (a) a bundle of 180 NbTi strands (b) the complete NbTi CICC (c) copper wire with similar diameter[10]

4 Electrical Properties

Niobium as well as titanium are both metals, thus NbTi is also a metal compound, with a body-centered-cubic crystal structure. This BCC crystal has a got relatively small dimension, a scientific obtained value of about 329 nm. This means that the electrons and nuclei of adjacent atoms act upon the electrons from neighboring atoms. The distinct atomic states will split into closely spaced electron states, which will eventually form an electron energy band.[11] The structure of this band determines the electrical properties. In NbTi the outermost band is only partially filled with electrons leaving available electron states above and adjacent to the filled states. This means that only little energy is needed to move the electrons to empty states. If an external voltage is applied a large number of electrons will be moved to the conducting states, and NbTi will become conductive. And since NbTi is a superconductor the electrons will have zero resistance if the material is cooled below a certain critical temperature. More about that is discussed in the section about magnetism and superconductivity.

The superconducting magnet coils in ITER will be built of Cable in Conduit Conductors (CICC) of NbTi and copper. In which strands of NbTi and copper will be present. Because of this the critical current is a very important property. When a current that is flowing in a superconducting wire is increased the magnetic field strength at the surface of that wire is also increased, until this magnetic field reaches its critical value. If that happens the sample that is worked with at that moment is returned to its normal state. The current that runs through the wire just before this happens is called the critical current. Since the magnetic critical field strength decreases if the temperature is increased and since the critical current is proportional to the magnetic field, the critical current will also decrease if the temperature is increased. However for the ITER project the temperatures of the cables are low.

Measurements on the dependence of the magnetic field on the critical current have been done on NbTi wires of 34 wt% Nb and 66 wt% Ti.

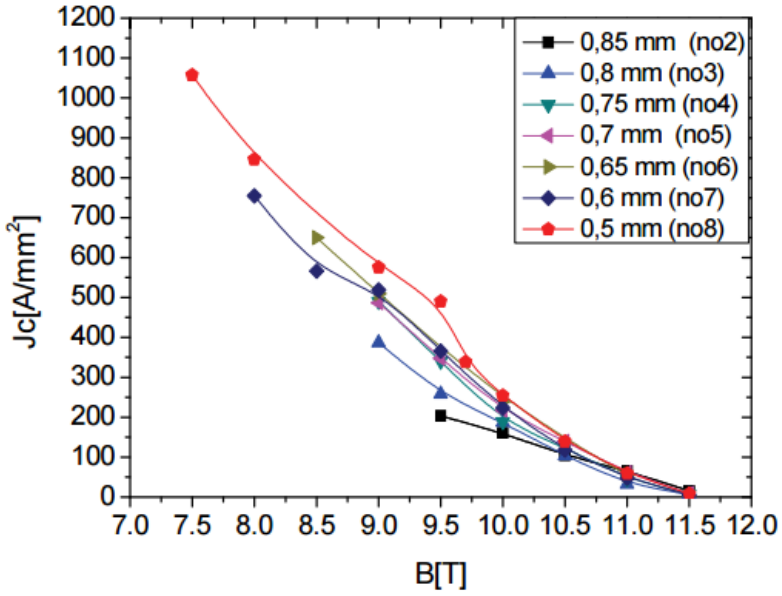

Figure 4.1: Dependence of the magnetic field on the critical current.

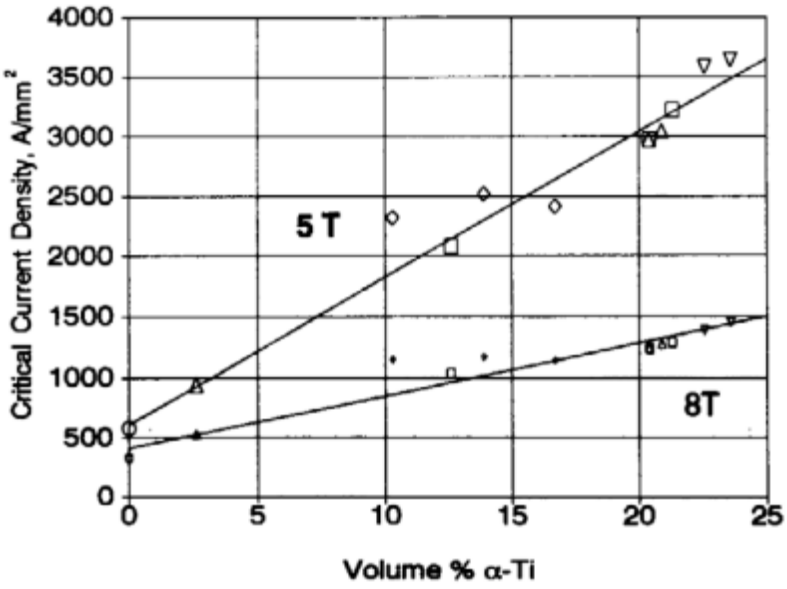

Figure 4.2: Influence of volume % α-Ti on the critical current.

Seven different samples were made from this wire by using cold drawing with the following diameters: 0.85 mm, 0.8 mm, 0.75 mm, 0.70 mm, 0.65 mm, 0.60 mm, 0.50 mm. The measurements were made in a temperature of 4.2 K. Results can be seen in *Fig.* 4.1.[12] Note that when the diameter of the wire decreases the critical current increases with a considerable high amount. This is probably because of the forces applied with cold drawing increases the grains boundaries in the wire, and it also improves the connections between filaments. Other measurements, with the same samples, of the influence of cold drawing on NbTi have proven that the critical temperature and the critical magnetic field do not increase.

In the NbTi wires there exists α-Ti precipitations, these are of great influence on the magnitude of the critical current. This gives also a way to control the critical current. For example

by messing up the microstructure with cold working and heat treatments.[13] In *Fig.* 4.2 the influence of these α-Ti precipitations on the critical current can be seen.

As said the magnet coils are built of cable in conduit conductors. The manufacturing of these cables can cause some deformations on the single NbTi wires. Examples are small indentations because of the wrapping, flattening or pinching. Also possible are defects at the outer cable due to compaction processes. These defects might be of influence on the critical current. To see what this influence possibly is an organization involved in the manufacturing of the CICCs for the magnets that will be used in ITER performed an experiment on this topic.

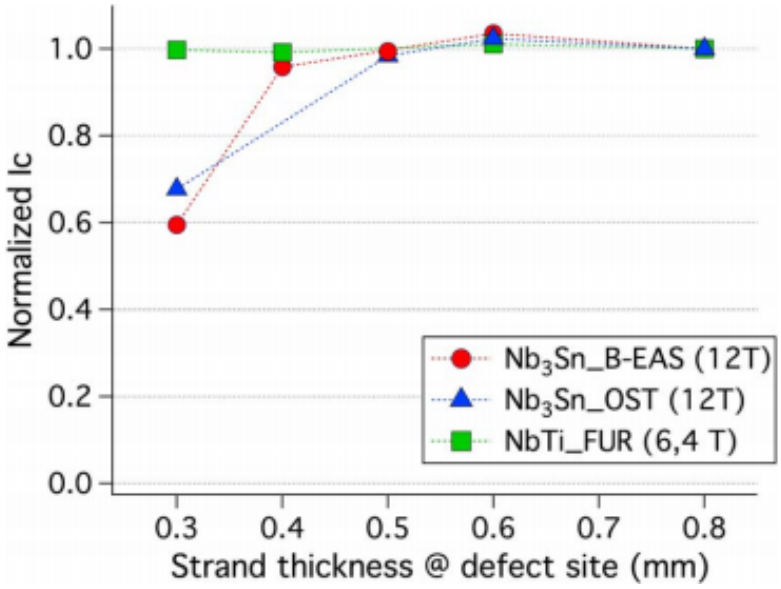

Figure 4.3: Critical current as function of the strand thickness.

They took strands from real CICCs and rolled different wires to different thicknesses, varying from 0.3 to 0.8 mm. They did this experiment for Nb_3Sn and NbTi samples. Next they measured the critical currents of the wires. The measured critical current values as a function of the strand thickness can be seen in *Fig.* 4.3.[14] Since for the purpose of this study only NbTi is of importance the results of Nb_3Sn are ignored. One can immediately see that the critical current of NbTi is not affected by the strand thickness at the defect sites (the green data points), which is a positive result for the ITER project.

In the end the electrical properties of NbTi are very promising for the ITER project. First of all it is a conducting material. Secondly the critical current increases when the diameter of the NbTi wire is decreased, under a certain magnetic field. Also the critical current can be controlled because of the α-Ti precipitations in the NbTi. And thirdly when the NbTi wires are twisted to form the CICC structure there will form some defects, however the critical current is not affected by these defect sites and the thickness of the wire on that point.

5 MAGNETIC PROPERTIES

For the purpose of this report this section will cover magnetic properties at low temperatures only as this is were NbTi becomes superconductive.

Niobium Titanium is an essential supermagnet workhorse as it is a metal which can withstand great electric current densities and does not dissipate in the presence of a large magnetic field. It is economical and convenient to refrigerate as it remains superconductive at high enough temperature. In addition to this NbTi produces two phase nanometer scale microstructures which can be processed into a large number of complex filament composites while the possible length of a strand remains in the kilometer region. It must however be stated that it is mainly the ductility and simplicity of fabrication that makes NbTi an outstanding material as there are many other materials with far superior superconducting properties.

The superconductive properties can currently be best exploited using fine filaments of a NbTi alloy embedded in a copper matrix this results in less diamagnetism and greater stability. Both the rate of change and the amplitude of the magnetic field are advantages of NbTi supermagnets. The discharge period of common laboratory magnets is only a few minutes. Magnets may be wound both with multifilamentary NbTi conductors as well as single filaments. The use of single filament NbTi magnets is commonly in nuclear magnetic resonance measurements where stability of the magnetic field over long periods of time is essential. The time required to charge single filament NbTi magnets is longer than that of multifilamentary wound magnets but this becomes insignificant when the field can be held constant for long periods of time.

In order for these filaments to be useful for superconductive purposes they must contain fine α-Ti precipitates. In conventional strands these alpha precipitates function as the main flux pinning centers making their optimization a goal of the complex fabrication process. The shape of these α-phase pins is constrained to a ribbon-shaped pin morphology by the plane strain deformation dynamics of the body centered cubic β-Nb-Ti and can be seen in *Fig.* 5.1.[15]

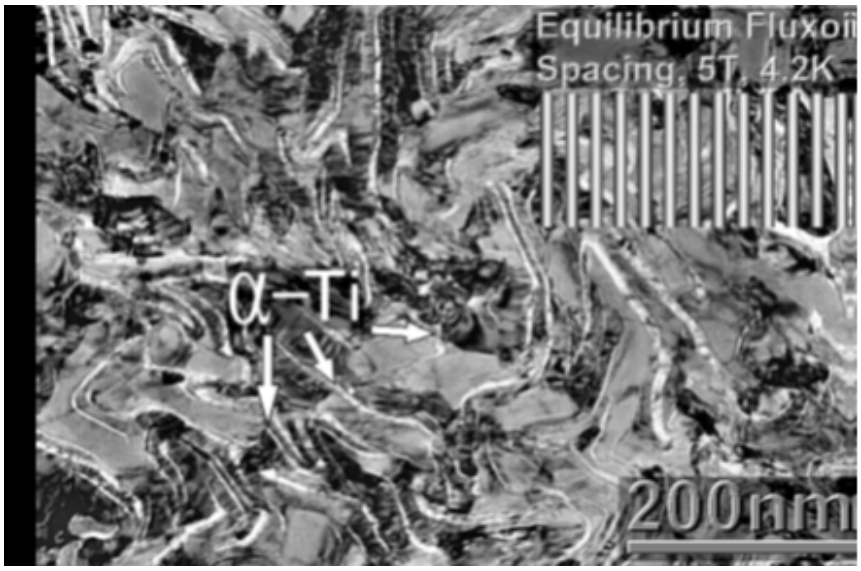

Figure 5.1: Typical Nb-47wt%Ti high critical current microstructure (in transverse cross-section) showing the densely folded sheets of α-Ti pinning centers dispersed within the superconducting α-Nb-Ti matrix. Superimposed is a schematic illustration of the equilibrium fluxoid spacing and dimensions appropriate to Nb-47wt%Ti at 5 Tesla, 4.2 K.

It is possible to predesign the desired pinning by mechanically assembling the structure to be acquired in a large composite and the using methods such as multiple extrusions and wire drawing in order to reduce the structure to the dimensions of the fluxoid lattice. This is called Artificial Pinning Centers (APC) and provides great versatility in the selection of pinning and thereby allows for great optimization for the desired application. The geometry of the pinning centers can be modeled and simulated to find the perfect setting. Furthermore there is great flexibility when it comes to the superconducting matrix. The grand issue using this approach is that the idealized macrostructure of the large composite is not exactly the same as the final size nanostructure. Since APC commonly requires multiple extrusions, which each only have a maximum yield of 85 percent, it is obvious that a design requiring more than 3 extrusions has a very poor effective yield. The fact that the composite is two-phase from the very large beginning of fabrication does not aid the process as this may lead to work hardening or even fracture. This does not always have to be the case but definitely makes APC wires break more commonly than conventional wires.

A very valuable optimization parameter of NbTi strands is the Volume Flux Pinning Force given by:

$$F_p = J_c * B \tag{5.1}$$

This Volume Flux Pinning Force is mainly influenced by the size of the wire and its precipitates. NbTi's volume flux pinning force behaves very strangely and unlike most other high field superconductors making NbTi so effective near its upper critical field. The maximum of this force occurs at about half of the upper critical field and drawing the wire to its optimum size increases this forces at all fields. Furthermore it is important to note that, just like the critical current density, this force is linearly dependent on the volume percentage of pinned material.

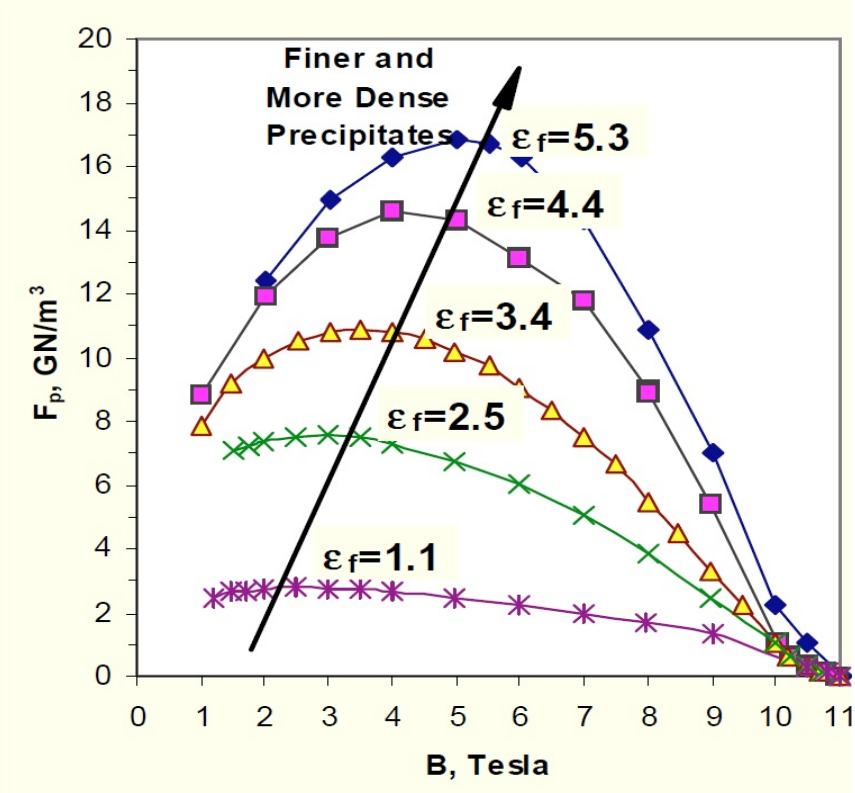

Figure 5.2: For conventionally processed NbTi the Volume Flux Pinning Force increases in magnitude with drawing strain after the final heat treatment. The increase occurs at all field as the precipitate size and spacing are reduced to less than a coherence length in thickness.[16]

For optimal properties the strands of NbTi embedded in copper must be twisted around other wires in a certain manner. This is required in order to reduce flux-jump instability caused by varying external fields and to reduce eddy-current losses. To ensure the twisting is locked it is advisable to be applied just as the multifilamentary strand has reached its final size. In general it can be said that the higher the magnitude of the rate of change of external field the tighter must be the twisting.[8] The twist pitch of the wires strongly influences the coupling loss which is the reason why ITER deployed a R&D group specifically to find a strand which addresses the degradation issues commonly found in untwisted strands. The final coupling loss of the wires is not only determined by the absolute value of the pitches but also the ratio between the lengths of consecutive cabling stages. When the ratio is close to 1 for the twist pitches between consecutive stages, excluding the last pitch with high resistive wraps, it is found that the coupling loss can be significantly reduced. A lot can be understood about this mechanism by looking at the trajectories of the strands at their base. When the pitch ratio is close to 1 the linked flux is reduced as the strands form narrow loops. Currently the final coupling loss can only be predicted with a large range of error as the inter-strand contact resistance cannot be accurately stated. To fully analyze the system one must also account for the influence of cable stiffness related to the void of fraction and cable pattern, which can be deduced from experimental data.[18]

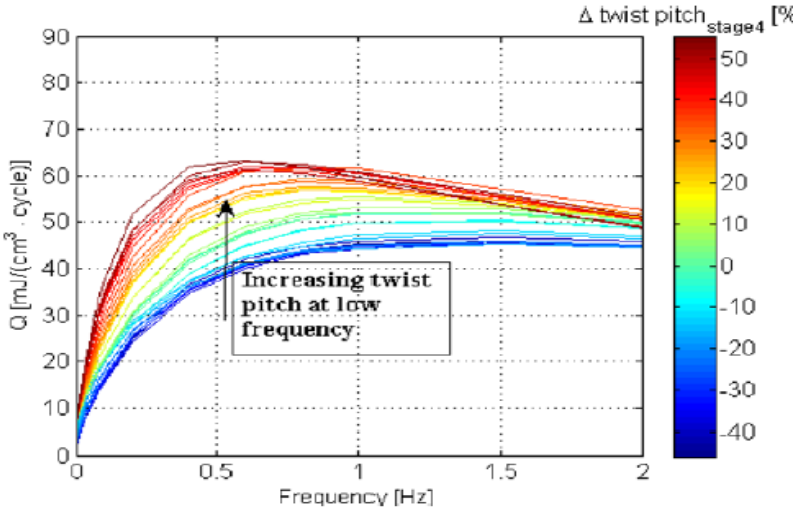

Figure 5.3: Effect on coupling loss of the variation of the twist pitch of stage 4 for the 131-161-241-296-453 mm sequence. The colored bar shows the percentage of applied elongation with respect to the nominal value.

One of the most common applications of NbTi is medical magnetic resonance imaging machines (MRI) were intense magnetic fields are required at almost all time. Due to the fact that electric current can run through a supermagnet without resistance these MRIs' magnetic fields are generated using superconducting electromagnets. The essential idea behind using supermagnets instead of conventional copper wound electromagnets is that the input energy required to operate a supermagnet, which mainly consists of cooling the material to a couple of Kelvins, is far lower than the energy required to counter the resistance within a conventional electromagnet. This refrigerant temperature for a common strand of NbTi is 4.2K.[19] To achieve this low temperature liquid helium is used as a coolant and typically a field of 9 Tesla can be achieved. A typical MRI scanner requires about 1,700 liters [20] of liquid helium to remain cooled close enough to absolute zero in order to reduce the resistance in the wires to nothing. Regardless of being the second most abundant material in the universe Helium is running scarce on earth as it is not bound to our atmosphere and constantly being lost to space. New technologies under the label *Cryogenics* allow standard MRIs to be cooled using only a small amount of liquid helium and a compression & expansion process which ensures the helium gas to remain cold and not condense into a liquid. These new methods reduce the dangers of handling the cold liquid nitrogen and do not require as highly trained personnel. Cryogenic techniques may also be used for detecting particles in calorimeters by keeping heavy gases such as argon and krypton in a liquid state.

Some other applications of supermagnets include the Tevatron, the Large Hadron Collider (LHC) and ITER. These use the other advantages of supermagnets in large high-energy particle-beam accelerators to bend charged-particle beams and plasma. The LHC is one of the largest cryogenic systems in the world which means it is a system based on running on very low temperature but achieving high performance. The main magnets in the LHC operate at 1.9K creating a current of 11,850 ampere to produce a magnetic field of 8.33 Tesla around its 27-kilometer ring.[21] Cooling is provided by a closed liquid-helium circuit based on cryogenic techniques. The LHC magnet cooling process utilizes three steps: refrigerating helium down to 80K by use of liquid nitrogen, then 4.5 K by use of turbines and finally 1.9K by use of special 1.8K refrigeration units. If helium is cooled below 2.17 K it transfers from a liquid to a superfluid state. This state has incredibly useful properties such as high thermal conductivity and makes it an ideal

coolant for the LHC.

The superconductive application which is most fascinating for the public seems to be the Maglev trains which travel at commercial speeds of up to 430 km/h. These advanced vehicles are the cutting edge of the railroad industry. Magnetic forces are used to levitate the technology, preform propulsion and provide guidance. The optimal design is a combination of environmental friendliness, advanced technology and the economics of the project under question. [22]

Most commonly superconductivity is used to exploit the zero DC resistance as this is routinely used in science, research and development as well as medical diagnosis. However the ultra low AC losses may also be conclusive in possible energy savings, demonstrations of power and current limiters. *Quantum interference effects* within superconductive materials allow us to monitor tiny magnetic fields which enable us to successfully record functions of the brain and heart.[23]

One of the most advanced superconductive systems is the International Thermonuclear Experimental Reactor (ITER) which uses superconductive strands of Niobium Titanium as well as other superconductive materials such as Niobium Tin to confine charged particles within a plasma, shape the plasma and generate the necessary vertical plasma stability. The major plasma in the ITER magnet system has a radius of 6.2 m, a volume of 840 m^3, 15 mA current and a fusion power of 500 MW. It is accepted to expect the first proper results of running the ITER by 2025.[24] The cable-in-conduit conductors (CCICs) of the ITER central solenoid will carry currents up to 45 kA in magnetic fields exceeding 12 Tesla. Due to this all strands used within the ITER will experience very significant electro-magnetic loads because of the Lorentz Force. Axial and bending strains will be observed in the transition from heat treatment to operational temperature as the jackets and strands thermally contract. This strain may be avoided by properly engineering the twist pitches.

An important way to specify supermagnets is their homogeneity; most manufacturers specify this in terms of the width of the resonant signal at half the signal height. Another common method is to use a small volume NMR sample to measure the magnetic field at various points in the specified homogeneous volume. This approach allows for far better detection of variations at any point in the volume but still fails to reveal very small deviations. Homogeneous magnets with homogeneities of ±0.001% can be achieved with significant effort and deploying room temperature trim or energized superconducting coils. The routine homogeneity is about ±0.1% for one-centimeter diameter spherical volumes. In the late 1980s, with the discovery of underpinning, came a big jump towards high homogeneity NbTi alloys which immediately generated an unexpected rise in performance on an industrial scale of up to 50%.

To limit the rate of coolant boil-off due to constant feeding of current to the magnet, supermagnets are often equipped with persistent switches. These consist of a short superconductive wire connected across the input terminals of a magnet and an electrical integral heater. The nominal resistance of the electrical heater in a typical switch is 60 Ohms and requires 35 mA of current to drive a superconductor into its resistive state. In normal state the wire has a resistance of 15-20 Ohms.

The most valuable attributes of any supermagnet are its critical magnetic field strength, critical temperature as well as the critical current density. Another important criterion for conductor design and fabrication process is the magnet size. Commercial alloys of NbTi are often formulated for optimum critical field in a range of 46-50%wt Ti although optimal critical temperature

actually occurs toward the lower end of Titanium content. Optimal critical field and critical temperature of NbTi do not occur at the same composition because the non-superconductive state resistivity increases with %wt Titanium. As a result of the heat treatments during manufacturing a titanium-rich alpha phase is found on the dislocation cell boundaries which provide the majority of flux pinning. Optimal pinning would require the fluxoid spacing to be the same as the precipitate cell size. To prove that the Titanium content is the major contributor of pinning it is advisable to create a graph of the critical current density versus alpha phase Titanium content[25], this can be seen in Figure 4.2. The key parameters of critical magnetic field and critical temperature are essentially determined by the chemistry of Niobium Titanium. Critical temperature of a material in zero field is related to the superconducting energy gap by:

$$3.5k_B\theta_c = 2\delta(0) \tag{5.2}$$

Here kb is the Boltzmann's constant and delta(0) is the energy gap at zero degrees. For type II superconductors it holds in the *dirty limit* where temperature and current density are zero that the upper critical field is given by:

$$B_{c2}(0) \approx 3.1 * 10^3 \gamma p_n \theta_c \tag{5.3}$$

Here γ is the Sommerfeld coefficient of electronic specific heat and p_n is the resistivity in the normal state. The upper critical field of NbTi at 4.2 K is about 10.5 Tesla, this can however only we reached with near perfect processing which is commonly not the case.

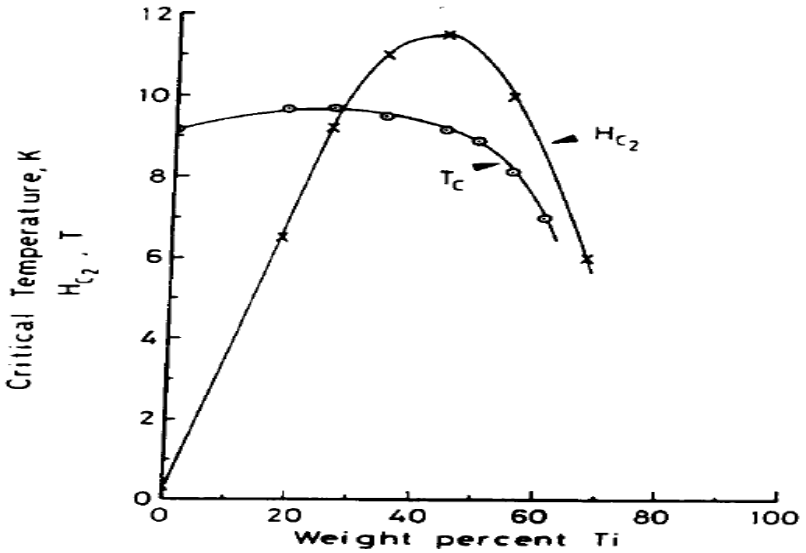

Figure 5.4: The critical temperature and upper critical field of NbTi at 4.2K as a function of alloy composition [26].

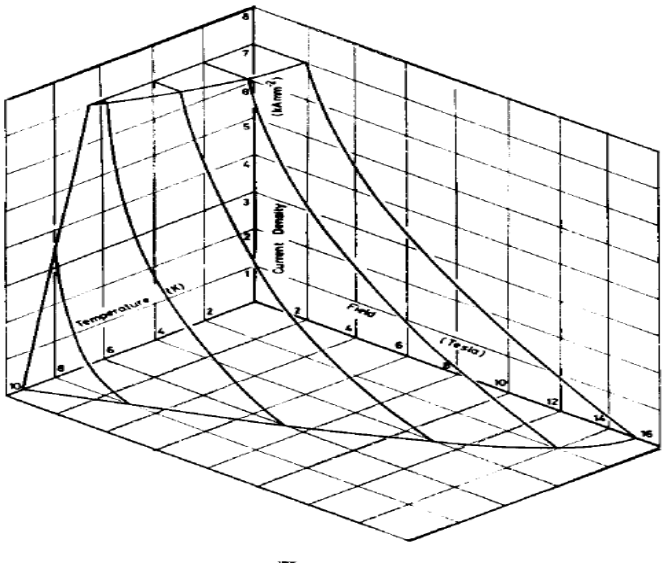

Figure 5.5: The critical surface of Niobium Titanium: superconductivity prevails everywhere below the surface and normal resistivity everywhere above it [25].

When operating supermagnets at higher temperatures or greater magnetic fields than specified the material may quench, causing both electrical and mechanical stresses in the windings. The wires within the electromagnet stop being superconductive and generate a lot of excess heat which may quickly lead to the defeat of some superconductive materials. Heat also means that the coolant surrounding the wires will quickly boil off. This in turn requires further amounts of liquid helium to be implemented into the system to recover the temperature change. As quenching is also a common issue in MRIs it has been found to be avoidable by adjusting the cooling method to advanced cryogenics. When discussing Niobium Titanium superconductive wires degradation may occur at low currents which lead to intense heating locally but also a spread to other parts of the windings. All stored energy of the magnet dissipates rapidly. To avoid this, the superconductive material has to be brought into direct contact with a good conductor such as copper in order to improve local cooling as well as ensure that the coolant is in close contact with every conductive wire.

6 Optical Properties

Optical Properties of a material are important to take into account when studying especially electrical properties of that material, because the two properties are linked. Knowing the optical properties enables someone to investigate further into the electrical properties, for example the concentration of conduction electrons and the Fermi surface can be derived.[30] The refractive index of a material is probably the most important parameter here; from it, conclusions can be drawn regarding the energy band structure.[29] It is a dimensionless number which describes how light travels through a material, a relation between the incident and the emerged or refracted beam.

When speaking about light interactions of a metal, three types need to be mentioned, namely transmission, absorption and reflection. When light interacts with a solid, so in this case with NbTi, the light can therefore be either transmitted, absorbed or reflected. It follows that the three mechanisms make up the total intensity of the incident light beam[27]:

$$I = I_A + I_T + I_R \tag{6.1}$$

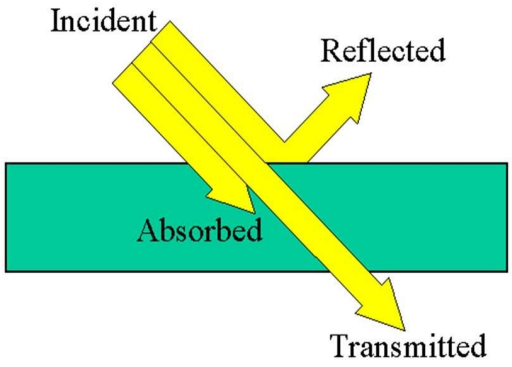

Figure 6.1: Schematic drawing of the three mechanisms.[28]

Results of measurements of these three types of light interactions for a material gives an overview of the optical characteristics, but the absorption is even more important. From it, the refractive index can be determined, using the Kramers-Kronig relation. This represents how the refractive index of niobium for example has been determined in the past (e.g. by Golovashkin et al. 1968). However, it turns out that very little research has been done on optical properties of NbTi as an alloy, but on Niobium itself. Therefore, the properties are first examined for the individual distinct elements, then conclusions are drawn for the alloy.

Experiments were carried out by Weaver, Lynch and Olson already in September 1972[29] in order to determine the optical properties of Niobium. Three different kinds of apparatus were used, namely a calorimetric technique in the infrared spectrum to determine the absorptivity at 4.2 K (which is the most interesting temperature for the application here) and a 15° angle of incidence, synchrotron radiation in the ultraviolet spectrum at room temperature to determine reflectivity from 5 to 36.4 eV at 10°, 45° and 60° and a spectrophotometer for the energy range of 0.7 to 6 eV.

The results for the absorptivity from 0.1 to 6 eV are shown below:

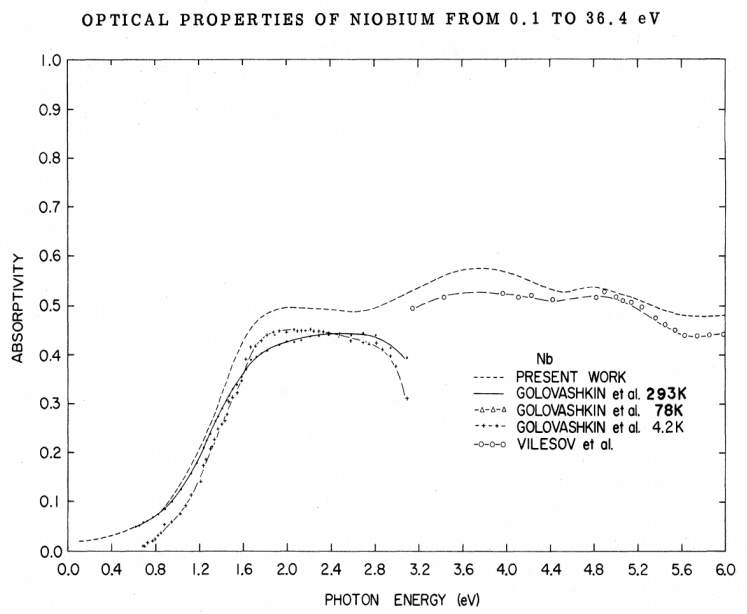

Figure 6.2: Absorptivity of niobium at 15° incidence angle (Present Work). Further, data from previous calculations is plotted as well.[29]

It can be seen that absorptivity increases greatly over a range from 0.1 to around 1.8 eV. However, it remains in a more constant range of 0.1 for the rest of the spectrum. In the article it is furthermore discussed where the different results in the region around 2.8 to 3.2 eV is coming from and a conclusion is drawn, that sample preparation was different in these cases.

In *Fig.* 6.3, the complete reflectivity spectrum in the range from 0.1 to 36.4 eV is shown. Noticeable is the drop of 50% reflectivity at 2 eV, followed by a shoulder at 2.6 eV, further decrease and increase again at 3.8 eV with a clear hump at 5.8 eV, followed by an almost smooth drop to a minimum at around 10.3 eV. Noticeable as well is the smooth decrease after the hump at 16 eV.

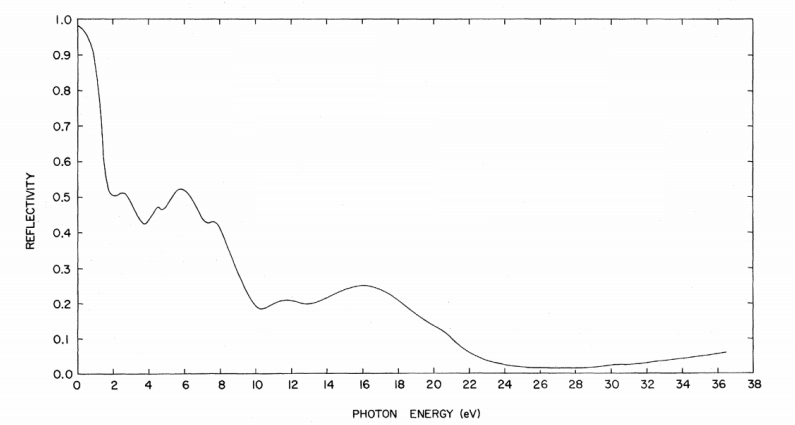

Figure 6.3: Reflective Spectrum of Niobium.[29]

From these two results it can be seen that up until 2.0 eV of photon energy, most of the incident light first gets reflected, then while increasing the photon energy, reflectivity decreases and absorptivity increases. While reflectivity is then fluctuating in the range from 2 to 6 eV, with a minimum at 3.8 and a maximum 5.8 eV, absorptivity remains in a range of 0.1. Generally speaking, reflectivity then decreases while increasing the photon energy.

A different set of experiments from July 1968 from Golovashkin et al.[30], investigation into the optical properties of Niobium in relation to its electrical properties was the goal. The refractive index has been determined at 4.2 K, the results can be seen in *Fig.* 6.4. In the long wave region, the refractive index increases monotonically with the wavelength of the light beam. In the short wave region around 0.4 to 2.8 μm, a maximum at 0.5 and at 2.2 μm appears, which was also noticed at room temperature.

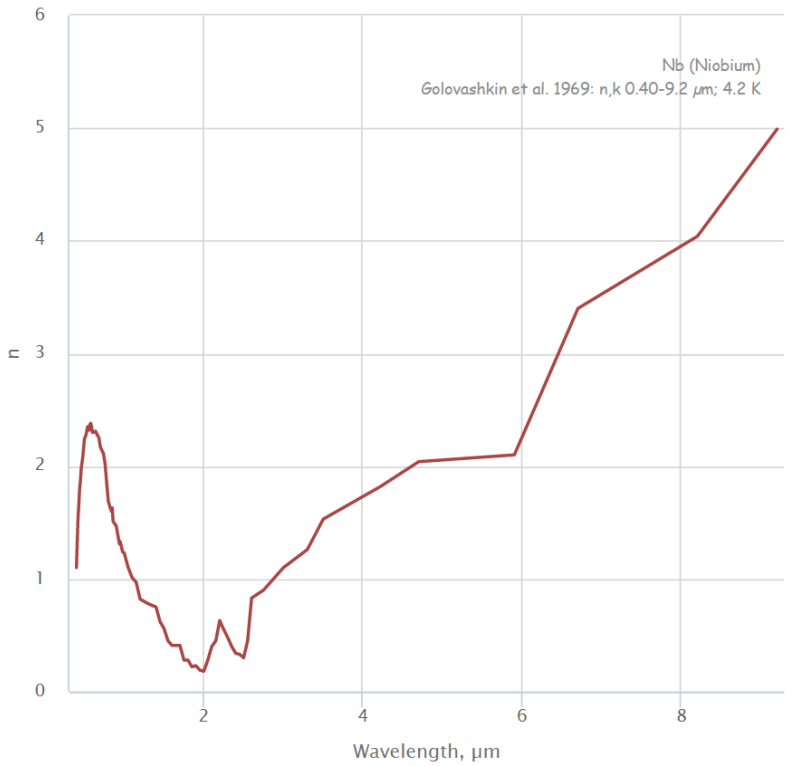

Figure 6.4: Refractive index of Niobium at 4.2 K.[30]

The paper concludes that Niobium has two principal bands of interband conductivity, the first one with a maximum at 4.0 eV and the second with the maximum at 2.5 eV. This can also be seen in the band diagram from Jani, Brener and Callaway (July 1988)[31]:

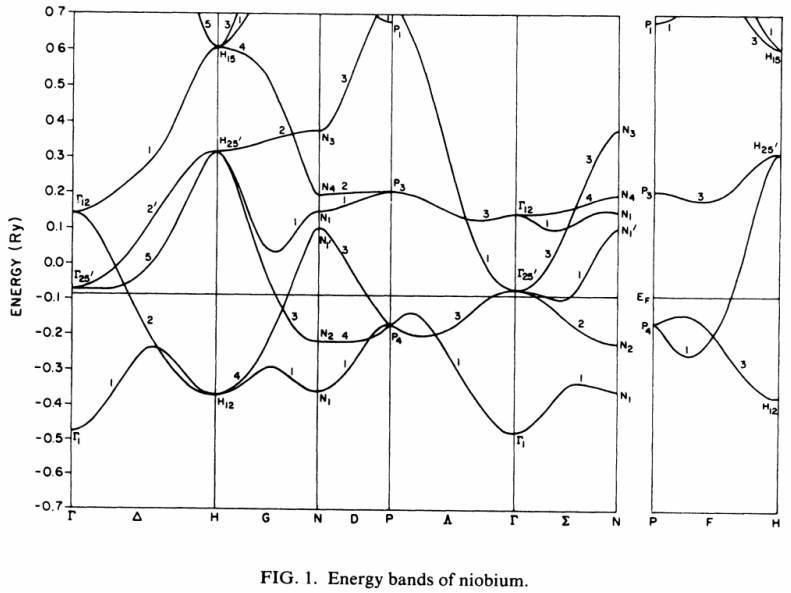

FIG. 1. Energy bands of niobium.

Figure 6.5: Energy bands of Niobium.[31]

Notice that the energy axis is in terms of the Rydberg constant. The 4.0 eV level corresponds to 0.29 Ry and the 2.5 eV level to 0.18 Ry. The overlap of the levels at these points can be clearly seen.

As previously mentioned, little research has been done on the optical properties of NbTi, and also the studies on titanium are mostly focused on titanium dioxide thin films or similar structures, which is not relevant for us. Titanium and Niobium are very similar elements with similar structures, since the ionic radius of both is similar and both are BCC structures. Therefore, we assume comparable optical properties for titanium and further, of niobium-titanium.

7 Synthesis Techniques

The superconducting magnets utilized in ITER are known as Cable-In-Conduit Conductors (CICCs). These are strands of superconducting material and copper which are twisted together and inserted into a jacket or conduit, usually made of steel. The configuration and ratio of superconducting to copper wires varies depending on its design characteristic and fabrication requirements. However the fabrication process remains consistent, namely a combination of direct extrusion and cold-drawing process for the creation of the superconducting high current carrying strands and pull through technology for the twisting and insertion into the conduit. The jacket itself it made using welding processing and cold work. This section of the paper will cover the specifics of design, development and fabrication of Niobium-Titanium CICCs for use in fusion reactors currently under construction.

7.1 Making a Superconducting Strand

Before any kind of wires can be inserted into any kind of jacket the strands that make up the wires have to first be produced. *Fig.* 7.1 depicts a paraphrased flow chart of the entire process. First of all one takes a rod of niobium-titanium and it in a copper extrusion can.[24] Then using hot extrusion this billet is pressed into a much thinner longer shape. Extrusion is a metal forming process in which a piece of certain length and cross-section (the billet) is pressed and forced through what is known as a die of a smaller cross-section thereby making the initial billet be formed into a shape and size.[32] One can perform either hot or cold extrusion however in case hot extrusion is used which has the advantage of allowing the metal to be moved around more

easily which allows vacancies to be filled up and impurities, which initially tend to cluster and form weak spots, to spread out.[32] The result is a single core rod with the niobium-titanium surrounded by copper. This is then pressed and shaped into a hexagonal shape. Multiple of these single core rods are then stacked together into yet another copper extrusion can which undergoes hot extrusion to yield what is known as a multi-core rod.[24]

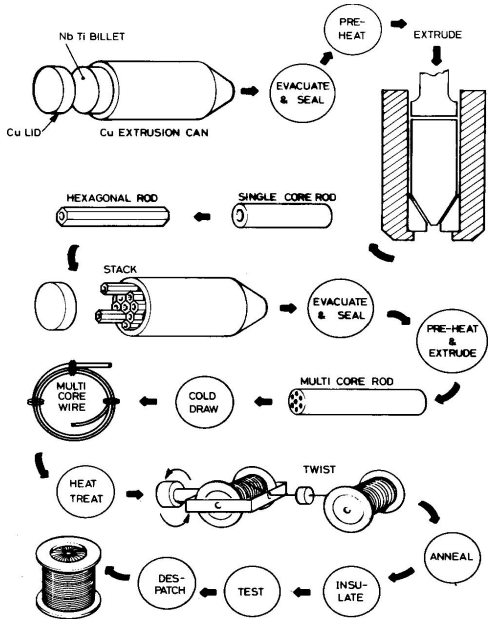

Figure 7.1: Production of NbTi CICC flowchart[24]

This multi-core rod then undergoes cold-drawing with intermediate annealing.[33] Cold drawing is simply another name for cold extrusion, as it is performed at room temperature. Annealing is a process by which the niobium-titanium is heated to a specific temperature and then allowed to cool slowly. This process of annealing followed by cold drawing, followed by annealing is done so that an α-Ti precipitate is formed and then spread into the proper shape. The annealing causes the precipitate to form yet it causes it to form large clusters with a thickness of 200-800 nm.[34] For reasons explained elsewhere in this paper the precipitate must be reduced to a much smaller thickness and by cold drawing it thickness becomes 1-5 nm and its shape and arrangement are also improved.[34] Once this is done one has obtained a multi-core wire, the details of which can be seen in *Fig.* 7.2. It is worth noting that after this entire process the strand thickness is incredibly small, 0.81 mm to be exact.[33] Additionally one must avoid the formation of brittle copper-titanium compounds during heat treatments as these obviously weaken the overall integrity and ductility of the final wire. As such the niobium-titanium is encased in a very thin niobium shell.[24]

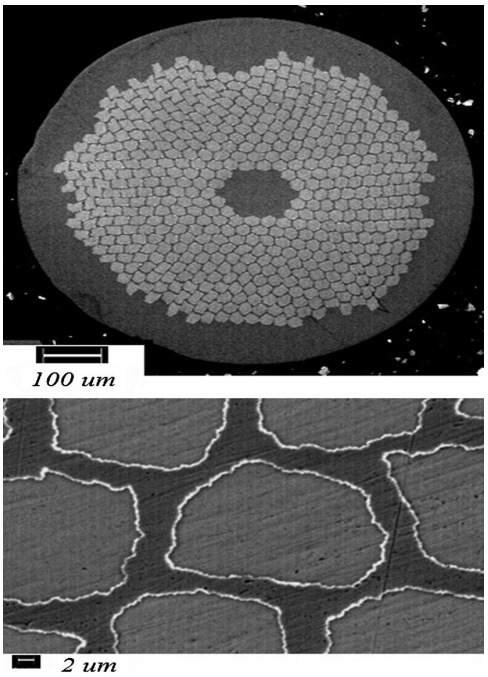

Figure 7.2: Close up of multi-core wire[33]

7.2 Cabling

Now that fabrication method for the strands has been detailed it is time to go one step larger, the cabling. This entails how these strands are combined together to form the best overall superconducting wire. A superconducting wire for use in fusion reactors such as ITER is never made purely of the strands discussed above; they are always combined with strands of pure copper. As one can imagine there are numerous ways one can combine superconducting strands and copper strands to create a superconducting cable, and each will have different properties including (but not limited to), upper and lower current limits and void fractions. For fusion relevant purposes it appears that the best cabling scheme is written as [(3+3)x2+2x6x4x6+(1x6)x4x4] [33] and can be seen in *Fig.* 7.3. From it, one can see that the final cable consists of 7 sub-cables and these in turn each consist of 4 sub-cables. The cabling stages are denoted from 1 through 5C and once a stage has been formed it is twisted to a certain twist-pitch to avoid coupling. Hence the final cable is 7 twisted together sub-cables each consisting of 4 smaller twisted together sub-cables each of which consist of 6 twisted together strands.

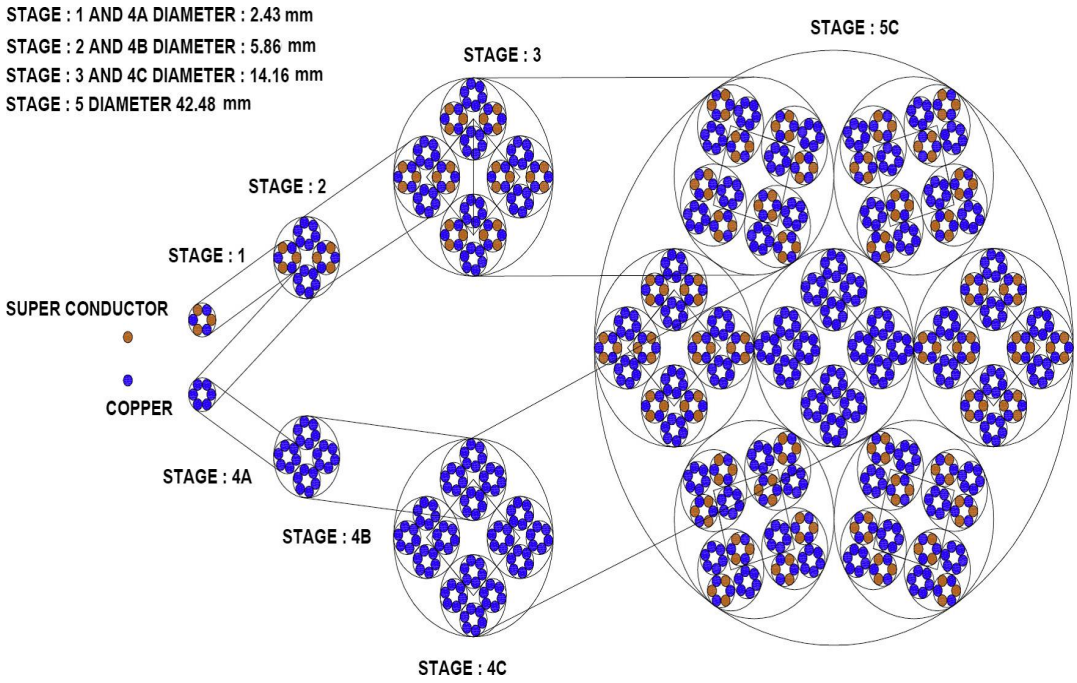

Figure 7.3: Ideal cabling layout for a CICC[33]

Through dummy copper strands the cabling parameters of the cabling facility have been optimized to give the best result. The stage 1 and stage 4A wires were twisted to a pitch of 36.0 mm, stage 2 and 4B wires to a pitch of 66 mm, stage 3 and 4C to a pitch of 121.5 mm and the final cable has a pitch of 260 mm. The final actual diameter of the cable was found to be 35.25 to allow for an easier insertion into the jacket.[33]

7.3 JACKETING

There are two methods through which the CICC can be jacketed. The first is to wrap the cable in a metal sheet which is then turned into a jacket through longitudinal weld. For the second approach short tubes are butt welded together into a long length conduit and inserting a wrapped cable into this. For the production of a fusion relevant CICCs the second method is utilized. While the overall complication does increase with CICC length it is foreseen that a specifically designed jacketing fabrication line for long length CICCs will act as a solution.[33]

This fabrication line is made up of seven sections, the first being the wrapping station. The second is known as the jacket tube station. The third is the welding station followed by an inspection unit and a circular compaction unit. The final two sections are a swaging and a spooling section.[33]

SS316LN is the material that is chosen as the jacket material because of (among other reasons) its cryogenic compatibility and high strength. SS316LN is composed largely of iron but is combined with a myriad of elements but chiefly nickel and chromium, which combined make up about 30% of the material.[33] The foil to be used is a material known as SS304 which is similar to SS316LN but with different composition ranges.
So first the foil is wrapped around the cable with a 50% overlap, afterwards the entire cable is pulled through all of the short tube sections of the jacket (which are mounted on a tripod support structure) by tying one end of the cable with a steel rope which is attached to a spool. The short tube sections of the jacket are then welded together after which the entire length of the CICC is circularly compacted reducing its diameter to 35mm from the original 38.1mm. Finally

the CICC enters the swaging unit whereupon it adopts a square shape of dimensions 30 mm x 30 mm.[33]
Through this entire method the creation of 100 meter of niobium titanium CICC has been successful.

8 Relation between Synthesis & Structure

From Process to Structure

During the process of making NbTi wires which is described before in this report, the structure of the NbTi filaments keeps changing. In this chapter we will explain what changes occur during different steps of the production.

Cold Drawing and Annealing

In NbTi a linear increase in critical current density is observed with volume % of α-Ti precipitate. This is because by introducing the precipitates, pinning defects and the refinement of grain size are introduced. These elements are key to the success of superconductors which make use of NbTi.[37] These α-Ti precipitates are introduced in the material using cold drawing and annealing.

The α-Ti precipitations appear as a result of annealing, however this very process makes α-Ti precipitations very big and thick (200 nm and 800 nm wide). The precipitations which are formed during the initial heat treatments have microstructures with a large variation in size. However, in order to obtain a good pinning centre, α-Ti precipitations need to have the same magnitude as the thickness of coherence which for this material is equal 5 nm or less. This problem is solved by the process of cold drawing which decreases the thickness of the precipitates to 1-5 nm. But the cold drawing of the NbTi wires will also increases the lengths of the precipitates, alter their shape from ellipsoidal into a strip, change their arrangement toward the flow of current, decrease the distance of α-Ti separations (3-6 mm), and it also enlarge the coiling and bending of the ribbons of α-Ti precipitations.

In the following article[38] it is shown that an intermediate annealed monofilament which is heat treated at an estimated prestrain of 5 did not have the well-developed equiaxed transverse-cross-sectional microstructure that is normally expected at this prestrain. The resulting inhomogeneous distribution of precipitates was still there after the final precipitation heat treatment. Fine intragranular Widmanstaetten precipitation were still observed in the strand heat treated with an estimated prestrain of 7 as well as the strand made from the intermediate anneal rod used in this research. For this higher prestrain material, multiple heat treatment however removed much of the inhomogeneity and resulted in a large volume of precipitate. In 1989 Lee et al. found that the amount of prestrain required increases linearly with weight % Ti. [4] It was finally found that a strain of 6 would be sufficient to produce homogeneous precipitation for a restricted heat treatment of a Nb 4 wt% Ti - 15 wt% Ta alloy monofilament which was treated in accordance with is illustrated in *Fig.* 8.1.

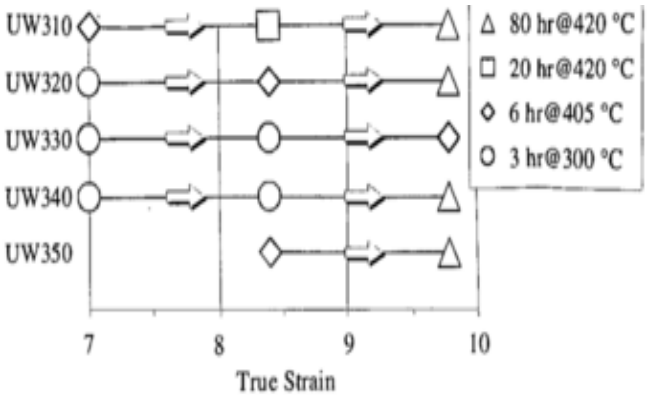

Figure 8.1: Schematic diagram illustrating the restricted heat treatment investigation of the Nb-Ti-15Ta alloy monofilament.[38]

The first heat treatment of the material will only yield approximately 10 volume-% precipitate, by applying additional cold work strain, the effect of the slow diffusion rate at these temperatures is again overcome and more precipitate is produced. To allow more precipitate to form, second and third heat treatments with additional cold work will be applied. These treatments typically yield 15 and 20 volume-% of α-Ti precipitate respectively.

The rapid temperature changes during the annealing process can cause material degradation, cracks and voids in the structure, shifts and dissipation of defects. By using the cold drawing process it is possible to repair these factors that had been lost or damaged.

If too little cold work is applied before the first heat treatment, Widmanstaetten precipitation (an example of a structure like this is seen in *Fig.* 8.2) will occur, causing increased hardness (reducing draw ability) and producing a non-optimum precipitate size and distribution.

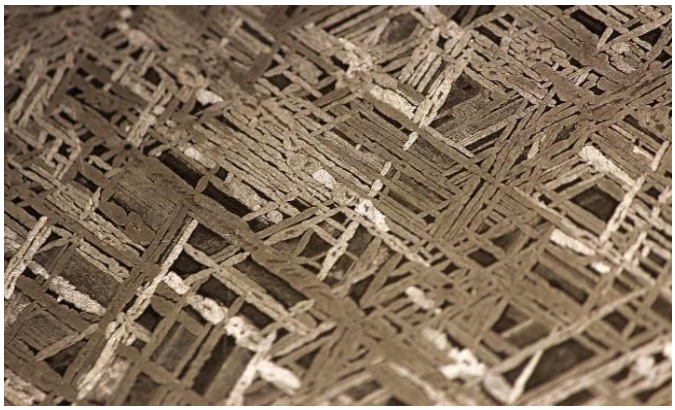

Figure 8.2: An example of a Widmanstaetten structure.

An alternative to the heat and cold treatments the pinning sites can also be introduced mechanically by hand-assembling the desired microstructure.
The cold drawing does not only change the shape of the precipitates. The NbTi grains are also affected by this process. They become elongated towards the drawing axis during the drawing. Due to the process of cold drawing the filaments diameter has decreased from 1 μm to 3 μm. The biggest diameter reduction was observed among filaments that were placed in the very middle of the wire, and the smallest diameter reduction occurred in the filaments that were far from the wire's centre.

Composition

The composition of the materials used will be of a big importance to the structure of the final material.

To obtain an optimal composition of the NbTi strands we start with an alloy of between 46.5 and 50 wt% Ti. If the amount of Ti is decreased within this range, less precipitation of the α-Ti phase will occur. This results in the increase of both the critical temperature and the upper critical current. A maximum of 11.5 T for the critical field is found at 44 wt% Ti for T=4.2 K. However the precipitation of α-Ti is desired for flux pinning and high critical density, so the amount of Ti also shouldn't be too low.

The composition of the NbTi also affects the morphology of the α-Ti precipitate, for low amounts of Ti the α-Ti is formed at grain boundary intersections. At these intersection the precipitate tends to be uniform in size and distribution, so it does not significantly affect strand ductility. If higher Ti compositions are used, fine distributions of Widmanstaetten-type precipitation are formed in the grain interiors. This will result in both a non-uniform microstructure and a significant hardening of the NbTi.

There also has to be made sure that the final alloy is free of unmelted Nb or non-ductile inclusions to avoid in filament and ultimately strand breakage, so enough Ti has to be added to the alloy to let all the Nb-ions react.

All these above factors are very sensitive to the composition so an optimal value of α-Ti has to be found from the starting point of *50/50* Nb/Ti.
Next to changing the composition of the NbTi alloy to improve performance, impurities can be introduced in the strands. The content of impurities used to be kept low, however recent work has shown that increasing the allowable content of iron can considerably refine the precipitate size without adversely affecting the precipitate volume.

Extrusion and Billet

The process of extrusion is widely used to produce ceramic components having a uniform cross section and a large length-to-diameter ratio, such as ceramic tubes and rods.

The process of extrusion is started with the hot forging of the NbTi ingot to the required diameter and then annealing in the single phase β region (approximately 2 hours at 870°C). For fine filament Cu matrix composites the NbTi ingot is then sealed inside a high purity Cu extrusion can. This can is succeedingly warm extruded this process results in a well bonded monofilament. The Billet assembly for this extrusion process is perfumed in a clean environment in order to avoid introducing particles that would not co-deform to the sub 0.05 mm filament size. If this would happen the final structure will be contaminated with large grains or particles.

The thickness of the Cu around the NbTi wire at this stage is important because it will finally determine the distance between two NbTi filaments in the final wire. It is preferred to have a filament spacing to filament diameter (s/d) ratio of 0.15 to 0.20.
For DC magnet application, it has been established by Ghosh et al (1987) that a minimum Cu thickness of 0.4 μm to 0.5 μm is required to reduce the magnetization which occurs between filaments which are adjacent.

Although warm extrusion would help bond the composite, as much of the processing as possible is performed cold by wire drawing, we discussed the need for cold drawing earlier in this chapter.

Twisting of Strands

To reduce flux-jump instability caused by varying external fields, and to reduce eddy-current losses the strands are twisted around its drawing axis. This twisting can be best applied just before a multifilamentary strand has reached final size so that the twist can be locked into place by a further die-pass. The higher the expected rate of change of field, the tighter the required twist pitch has to be.

Final Wire Drawing

The final stage of the processing of the material used for the NbTi strands is wire drawing. However according to the extensive final wire drawing produces a plain strain condition in the BCC β-NbTi. This process will result in a reformation of the α-Ti precipitates throughout the material. The precipitates will rearrange themselves into densely folded sheets, see *Fig.* 2.2. This folding process rapidly decreases the precipitate thickness and the area between the different precipitates with a dependence of $d^{1.6}$ (where d is the strand diameter) and increases the precipitate length per area with a dependence of $d^{-1.6}$.[8]

As a result of this change in the α-Ti precipitates the critical current density will change. At first it will increase as the microstructure is refined until it reaches a peak, after which there is a steady decline. This peak in critical current density will occur at a strain of about 5 for a multifilamentary strand with uniform filaments. It is seen that it is important to have a uniform cross-section throughout the whole wire.[37]

This is because the amount of current that can be carried by an individual filament is reduced if the filament is locally necked to a smaller diameter. The current from this necked filament may be locally transferred to adjacent filaments, but there will still be a broadening of the critical current transition. With final filament diameters of less than 20 microns often required, this imposes a very high level of quality control on the processing of the strands. The degree of filament uniformity is reflected in the sharpness of the superconducting transition with increasing current. This means that for the filaments which are non-uniform in cross-section the peak in critical currents occurs earlier and at a lower critical current density.[37]

The most common source of a non-uniform cross-section is due to intermetallic formation or lack of bonding between the components of the composite. High performance strand (as in *Fig.* 8.3) have reduced these processes to a very low level resulting in a very uniform cross-section.

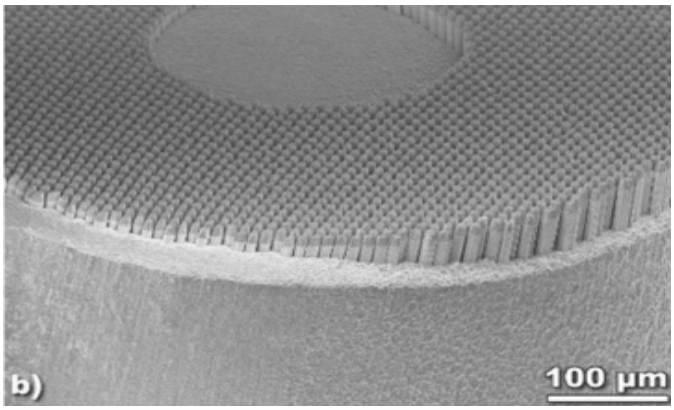

Figure 8.3: Etched cross-section of NbTi based superconducting strand fabricated by IGC-AS (now Outokumpu Advanced Superconductors) for the Interaction Region Quadrapole Magnets of the Large Hadron Collider at CERN.[37]

When drawing of the wire the ratio of matrix size to superconducting material does not undergo any changes. This factor is essential as it prevents the superconducting material from being destroyed.[36]
The final cross-section of the strand can be further controlled by die shape and size or by using independently adjusted rollers operating along the strand surface. In this way square or rectangular cross-section filaments can be produced. [37]

9 Discussion and Comparison

While NbTi is seen as the tried and true workhorse in the superconductor field, when very large fields are required it simply cannot be used. For such situations Nb_3Sn is utilized. This section of the report contains a comparison between the two materials including differences in structure, applications and to provide in a general sense what the main distinctive differences between the two are.

As is well known and discussed in detail in this paper NbTi is an easy to produce and manufacture material. Moreover it is extremely cheap costing roughly 300 USD per km depending on wire diameter or 100 USD per kg.[40] Due to its ductility there is an extremely large range of choices one can make to ensure the wire suits their superconducting needs including size, copper proportion, mono or multi filamentary to name a few. A wire with a diameter is 0.5 mm had a critical current of 500 A a critical current density of 2500 Amm^{-2} and at 4.2 K had a magnetic field limit of roughly 9.5 Tesla.[40] When cooled by superfluid helium down to 1.8 K magnetic fields of 12 Tesla can be reached, however, a lower temperature and higher field strength results in more energy being present in the wire and as a consequence the magnet might be irreparably damaged if it were to quench.[40]

Nb_3Sn is used whenever fields larger than 9 Tesla are required, as it has better critical characteristics, being able to maintain field strengths of 11 Tesla at a temperature of 10.4 K and critical current density of $10^6 Acm^{-2}$. Niobium tin is capable of reaching fields of up to 18T and is the main superconductor used at ITER where field strengths of 13 Tesla are needed. However, Nb_3Sn is by no means a wonder material as its mechanical properties are far from ideal. Due to its intricate structure of Nb_3Sn (as can be seen in*Fig* 9.1) is an extremely brittle material and therefore very resistant to bending or extrusion.

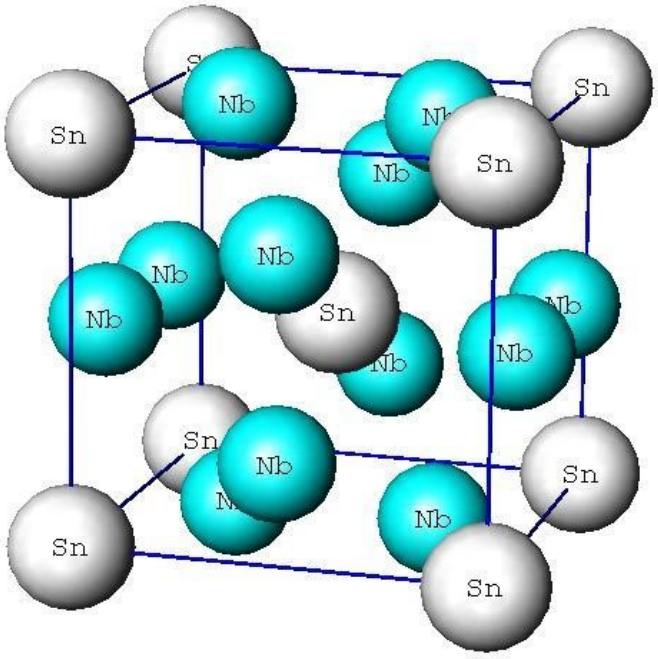

Figure 9.1: Structure of Nb_3Sn [41].

In figure we can see the structure of Nb_3Sn and it is quite unique. The tin atoms are arranged in a BCC structure while on each face for the unit cell two niobium atoms are situated in a centered manner, or in other words taking the front face as an example, they are aligned vertically

exactly halfway from the edge of the cell and horizontally they are each a quarter of the cell parameter from the edge. One can imagine that a structure like this is not prone to bending or stretching, especially when compared to the structure of NbTi wherein it makes absolutely no difference whether a niobium or a titanium atom inhabits a particular site. This makes Nb3Sn difficult to produce because the coil must be realized before any heat treatment is done whereupon it becomes very brittle. Having a cost of about 2000 USD per kg it is 20 times more expensive to produce than an NbTi CICC.

Practically speaking these are the main differences between a superconductor made from NbTi and one constructed from Nb_3Sn. Construction wise NbTi has cheaper materials and is significantly easier to wind, handle, and can be shaped for use in just about any situation. Nb_3Sn on the other hand is the superior superconductor able to maintain a magnetic field strength that roughly doubles that of NbTi (9 Tesla as compared to 18 Tesla). Hence when one needs a magnetic field larger than 9 Tesla one is left with little choice but find a way to make Nb_3Sn work, otherwise NbTi is the better alternative simply due to easy and cost effective production.

10 Conclusion

In conclusion NbTi is a tried and true material used for its superconductive properties. While not the best superconductor around it is the other properties that make it the currently most widely used material in this field. Produced through repeated extrusion in a copper billet to produce microscopic filaments encased in a copper matrix after which it undergoes a cycle of annealing followed by cold work to produce the necessary α-titanium phase in long thin ribbons throughout the NbTi filaments. The NbTi has a BCC crystal structure in which it makes no difference which sites are inhabited by niobium or titanium, it is simply pure determined by chance. Due to its ductility, which counter-intuitively improves at lower temperatures, it is easy to manufacture, handle, and can be custom made to suit a large range of applications. The variety of possible composites is great and allows for drawing into the kilometer range. It was learned that the critical current which produces the large magnetic field has an inverse relationship with the diameter of the wire due to increased grain boundaries and improved connection between the filaments. A proportional relationship with the percentage of the α-titanium phase present in the NbTi was also realized, this gives one control over the critical current and is due the messing up of the microstructure. A typical completed CICC strand of Niobium Titanium has a critical temperature of 4.2K at which a maximum field of 9 Tesla can be achieved. Lower temperatures are possible but not incredibly well spread as the costs of cooling increase drastically. Through an investigation of the optical properties of niobium and reasoning that NbTi must be comparable, it was seen niobium has two principal bands of interband conductivity one with a maximum of 2.5eV and one with maximum of 4.0eV. We reason that NbTi, if studied, will yield similar optical properties. Future applications of superconductive technology may be found in experimentation with near zero-AC losses and also the proposed project *DEMO* which is to become the first of a kind commercial station following the *ITER*.

Based on this report one may predict NbTi to remain the workhorse for MRI machinery as well as the up to date superconductive systems such as the LHC and ITER. However it must be stated that we believe it is unlikely for NbTi to have enough potential to compete with the currently more expensive materials with advanced superconductive properties such as Niobium Tin and YBCO. Given that their fabrication simplifies, costs are reduced and the materials are possible to be drawn to large lengths they will most certainly take over the market for high magnetic field appliances.

11 Acknowledgements

We gratefully acknowledge discussions with Arend Nijhuis, the University of Twente published papers he provided us with as well as his connection to some incredible Niobium-Titanium images.

12 REFERENCES

REFERENCES

[1] World Nuclear Association. (2015, November 30). Nuclear Power in Germany. Retrieved January 05, 2016, from http://www.world-nuclear.org/info/Country-Profiles/Countries-G-N/Germany/

[2] Nuclear fusion as a massive, clean, and inexhaustible energy source for the second half of the century: brief history, status, and perspective - Joaquin Sanchez - Energy Science and Engineering 2014; 2(4): 165-176 - Laboratorio Nacional de Fusion, CIEMAT, Madrid, Spain - DOI: 10.1002/ese3.43

[3] Conn, R. W. (2015, September 13). Nuclear fusion | physics. Retrieved December 15, 2015, from http://www.britannica.com/science/nuclear-fusion

[4] ITER. (n.d.). External Heating Systems. Retrieved January 10, 2016, from https://www.iter.org/mach/heating

[5] Delft, D. V., & Kes, P. (2010). The discovery of superconductivity. Phys. Today Physics Today, 63(9), 38-43. Retrieved from https://www.lorentz.leidenuniv.nl/history/cold/DelftKes_HKO_PT.pdf.

[6] Berlincourt, T. G. (n.d.). NIOBIUM-TITANIUM: WORKHORSE SUPERMAGNET MATERIAL. Retrieved December 15, 2015, from http://fs.magnet.fsu.edu/~lee/superconductor-history_files/Nb-Ti/Niobium-Titanium--Workhorse_Supermagnet_Material-2011.pdf

[7] Buga, S., Dubitsky, G., Serebryanaya, N., Kulbachinskii, V., & Blank, V. (2011). Superhard Superconductive Composite Materials Obtained by High-Pressure-High-Temperature Sintering. Applications of High-Tc Superconductivity.

[8] Lee, P. (2003). Superconducting Wires and Cables: Materials and Processing. Encyclopedia of Materials: Science and Technology, 1-11.

[9] Properties and Uses of Titanium. (n.d.). Retrieved January 26, 2016, from http://web-o-rama.net/titanium/1properties.html

[10] Wright, L. S., Wiederick, H. D., & Hutchison, T. S. (1984). Tensile test evidence of morphological structural changes in superconducting NbTi fibers and composites. Journal of Low Temperature Physics J Low Temp Phys, 57(5-6), 563-572.

[11] William D. Callister, JR., David G. Rethwisch. Fundamentals of Materials Science and Engineering, p.487, 4th edition, 2012.

[12] D. Gajda, A. Morawski, A. Zaleski, T. Cetner, A. Presz. Enhancement of critical current density in superconducting wires NbTi, 2011.

[13] ten Kate, H. (2016). Practical Superconductors for application in magnets. Presentation, University of Twente, Netherlands.

[14] R. Freda, S. Chiarelli, V. Corato, A. della Corte, G. De Marzi, A. Di Zenobio, A. Formichetti, L. Muzzi, A. Rufoloni, R. Viola. Performance Test of Superconducting Wires Subject to Heavy Deformations, 2015.

[15] 'NEW DEVELOPMENTS IN NIOBIUM TITANIUM SUPERCONDUCTORS', D. C. Larbalestier and P. J. Lee Applied Superconductivity Center, University Of Wisconsin-Madison, Madison, WI 53706 USA, 1996

[16] C. Meingast and D. C. Larbalestier, âĂIJQuantitative description of a very high critical current density Nb-Ti superconductor during its final optimization strain: II. Flux pinning mechanisms,âĂİ J. Appl. Phys., 66, pp.5971-5983, 1989.

[17] Lee, P. (2003). Superconducting Wires and Cables: Materials and Processing. Encyclopedia of Materials: Science and Technology, 1-11.

[18] Rolando, G., Devred, A., & Nijhuis, A. (2013). Minimizing coupling loss by selection of twist pitch lengths in multi-stage cable-in-conduit conductors. Superconductor Science And Technology, 27(1), 015006. http://dx.doi.org/10.1088/0953-2048/27/1/015006

[19] Americanmagnetics.com,. (2016). Characteristics of Superconducting Magnets. Retrieved 26 January 2016, from http://www.americanmagnetics.com/charactr.php

[20] Wired UK,. (2016). Cooling MRI magnets without a continuous supply of scarce helium (Wired UK). Retrieved 26 January 2016, from http://www.wired.co.uk/news/archive/2013-08/12/mri-magnet-cooling

[21] Home.cern,. (2016). Cryogenics: Low temperatures, high performance | CERN. Retrieved 26 January 2016, from http://home.cern/about/engineering/cryogenics-low-temperatures-high-performance

[22] Hamid Yaghoubi, Nariman Barazi and Mohammad Reza Aoliaei (2012). Maglev, Infrastructure Design, Signalling and Security in Railway, Dr. Xavier Perpinya (Ed.), ISBN: 978-953-51-0448-3, InTech, Available from: http://www.intechopen.com/books/infrastructure-design-signalling-and-security-in-railway/maglev

[23] Singh, A., Hussain, M., Singh, S., & Singh, R. (2004). FABRICATION OF MULTIFILAMENTARY NIOBIUM- TITANIUM SUPERCONDUCTING WIRE AND CABLE : TECHNOLOGICAL CAPABILITIES AVAILABLE AT ATOMIC FUELS DIVISION. BARC. Retrieved from http://www.barc.gov.in/publications/nl/2004/200405-3.pdf

[24] ten Kate, H. (2016). Practical Superconductors for application in magnets. Presentation, University of Twente, Netherlands.

[25] WILSON, M. (2010). ChemInform Abstract: Superconducting Materials for Magnets. Cheminform, 28(9), no-no. http://dx.doi.org/10.1002/chin.199709309

[26] Osamura, K. (1994). Composite superconductors (Chapter 5). New York: M. Dekker.

[27] Callister, William D. Fundamentals of Materials Science and Engineering: An Integrated Approach. Hoboken, NJ: John Wiley & Sons, 2005. Print. Chapter 19 - Optical Properties, Equation 19.4

[28] Torgerson, E. (2011). Light Day 1 Light and Reflection. Retrieved January 21, 2016, from https://etorgerson.wordpress.com/2011/05/02/light-day-1/

[29] Weaver, J. H., D. W. Lynch, and C. G. Olson. "Optical Properties of Niobium from 0.1 to 36.4 EV." Phys. Rev. B Physical Review B 7.10 (1973): 4311-318. Web.

[30] A. I. Golovashkin, I. E. Leksina, G. P. Motulevich, and A. A. Shubin. "The optical properties of niobium." Soviet Physics JETP 29.1 (1969): n. pag. Web.

[31] Jani, A. R., N. E. Brener, and J. Callaway. "Band Structure and Related Properties of Bcc Niobium." Phys. Rev. B Physical Review B 38.14 (1988): 9425-433. Web.

[32] Metal Extrusion. (n.d.). Retrieved January 26, 2016, from http://thelibraryofmanufacturing.com/extrusion.html

[33] Ghate, M., Raj, P., Singh, A., Pradhan, S., Hussain, M., & Abdulla, K. (2014). Design, development and fabrication of indigenous 30kA NbTi CICC for fusion relevant superconducting magnet. Cryogenics, 63, 166-173.

[34] Gajda, D., Morawski, A., Zaleski, A., Cetner, T., & Presz, A. (2011). Enhancement of critical current density in superconducting wires NbTi. Przeglad Elektrotechniczny, 87(6), 209-213.

[35] Enhancement of critical current density in superconducting wires NbTi. PrzeglÄĚd Elektrotechniczny, 87(6) - 2011, Daniel GAJDA, Andrzej MORAWSKI, Andrzej ZALESKI, Tomasz CETNER, Adam PRESZ

[36] Freda, R., Chiarelli, S., Corato, V., Corte, A. D., Marzi, G. D., Zenobio, A. D., . . . Viola, R. (2015). Performance Test of Superconducting Wires Subject to Heavy Deformations. IEEE Trans. Appl. Supercond. IEEE Transactions on Applied Superconductivity, 25(3), 1-4.

[37] Lee, P. (2003). Superconducting Wires and Cables: Materials and Processing. Encyclopedia of Materials: Science and Technology, 1-11.

[38] Lee, P., Fischer, C., Larbalestier, D., Naus, M., Squitieri, A., Starch, W., . . . Gregory, E. (1999). Development of high performance multifilamentary Nb-Ti-Ta superconductor for LHC insertion quadrupoles. IEEE Trans. Appl. Supercond. IEEE Transactions on Appiled Superconductivity, 9(2), 1571-1574.

[39] Greyloch. (n.d.). WidmanstaÌĹtten pattern. Retrieved January 26, 2016, from `https://www.flickr.com/photos/greyloch/14961451761`

[40] Donnier-Valentin, Guillaume. "Superconducting Magnets Theory And Design". 2011. Presentation.

[41] Geocities.jp,. "Crystal Structure". N.p., 2016. Web. 25 Jan. 2016.